Proceedings of PVP2008
2008 ASME Pressure Vessels and Piping Division Conference
July 27-31, 2008, Chicago, Illinois, USA

PVP2008-61205

NATURAL FLAW SHAPE DEVELOPMENT DUE TO STRESS CORROSION CRACKING

D. Rudland*, D.-J. Shim
Engineering Mechanics Corporation of Columbus
3518 Riverside Dr. - Suite 202
Columbus, Ohio

A. Csontos
US Nuclear Regulatory Commission
Office of Nuclear Regulatory Research
Mail Stop: T10-E10
Washington, DC 20555-0001

ABSTRACT

Typical ASME Section XI subcritical cracking analyses assume an idealized flaw shape driven by stress intensity factors developed for semi-elliptical shaped flaws. Recent advanced finite element analyses (AFEA) conducted by both the US NRC and the nuclear industry for long circumferential indications found in the pressurizer nozzle dissimilar metal welds at the Wolf Creek power plant, suggest that the semi-elliptical flaw assumption may be overly conservative in some cases. The AFEA methodology that was developed allowed the progression of a planar flaw subjected to typical SCC-type growth laws by calculating stress intensity factors at every nodal point along the crack front, and incrementally advancing the crack front in a more natural manner. Typically crack growth analyses increment the semi-elliptical flaw by considering only the stress intensity factor at the deepest and surface locations along the crack front, while keeping the flaw shape semi-elliptical. In this paper, a brief background to the AFEA methodology and the analyses conducted in the Wolf Creek effort will be discussed. In addition, the natural behavior of surface cracks under normal operating conditions (plus welding residual stress) will be investigated and compared to the semi-elliptical assumption. Conclusions on the observation of when semi-elliptical flaw assumptions are appropriate will be made. These observations will add insight into the conservatism of using an idealized flaw shape assumption.

INTRODUCTION

In October 2006, circumferential indications were located by ultrasonic testing (UT) in three of the pressurizer nozzle dissimilar metal (DM) welds at the Wolf Creek nuclear power plant. The indications located were relatively long circumferential defects in Alloy 82/182 dissimilar metal welds. In one case the flaw was sized at 43% of the circumference and 26% deep. Using ASME Section XI type analyses, Emc^2 and NRC staff estimated the times to both leakage and rupture for each indication. The results indicated that under certain conditions, no margin between leakage and rupture existed [1]. The results from these analyses led the NRC staff to request that the inspection/mitigation program currently in place for the pressurizer nozzles be accelerated. This acceleration affected nine PWR plants in the current US fleet. In response, the industry embarked on a short-term technical program aimed at refining the standard crack growth analyses conducted by Emc^2. The main emphasis of the industry program [2] was to use advanced finite element analyses (AFEA) to remove the semi-elliptical flaw assumption that is typical in ASME Section XI type analyses. In addition, detailed sensitivity analyses were conducted to demonstrate that sufficient margins exist for the pressurizer nozzles that would be affected by the accelerated inspection request.

In a parallel effort, Emc^2 and the NRC staff developed similar technology to confirm the results generated by industry [3]. In this effort a computer code, PipeFracCAE, was developed to conduct these advanced finite element analyses. This computer code, using the commercial code ABAQUS [4] as the solver, allows for planar arbitrary crack growth due to stress corrosion cracking. The natural development of the crack front is controlled by the stress intensity factor of each crack tip location along the crack front. A semi-automated approach is used to incrementally control the growth of the arbitrary crack front, see Figure 1. For PipeFracCAE, user defined crack growth laws, geometries, loads, and welding residual stresses can be added to the model via a user-friendly GUI and ABAQUS User subroutines. Extensive QA and benchmarking with the industry code FEACrack [5] were conducted in the aforementioned programs. The details of the PipeFracCAE software are given elsewhere [3].

* Corresponding author, drudland@emc-sq.com

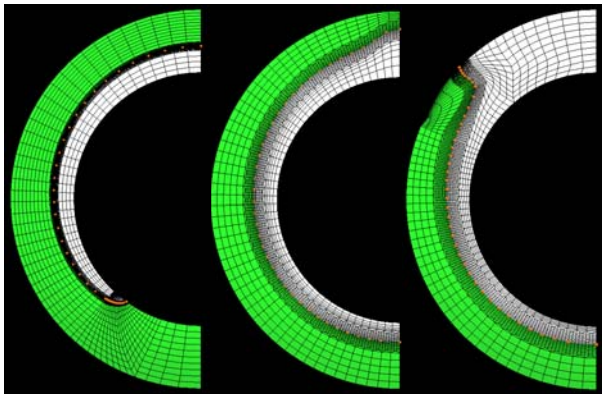

Figure 1 Examples of arbitrary crack fronts developed by PipeFracCAE

Using this software, the indication in the Wolf Creek relief nozzle was analyzed, and the crack shape prior to leakage is shown in Figure 2. In this figure, the dashed line represents the initial flaw size, while the solid line represents the flaw shape using the standard Section XI type crack growth analysis. For these analyses, the Anderson influence functions [6] for a semi-elliptical surface crack were used. In contrast, the circles represents the crack front generated using the PipeFracCAE software. The crack developed using the semi-elliptical assumptions just prior to leakage had a critical crack size margin (load at net-section collapse divided by applied load) less than one. However, when the natural crack shape was assumed (grown using PipeFracCAE), the resultant complex crack at first leakage had a critical crack size margin (again load at net-section collapse divided by applied load) of 2.6. In addition, when this natural crack penetrates the wall thickness, it becomes a complex through-wall crack, i.e., through-wall crack superimposed on a 360 degree surface crack.

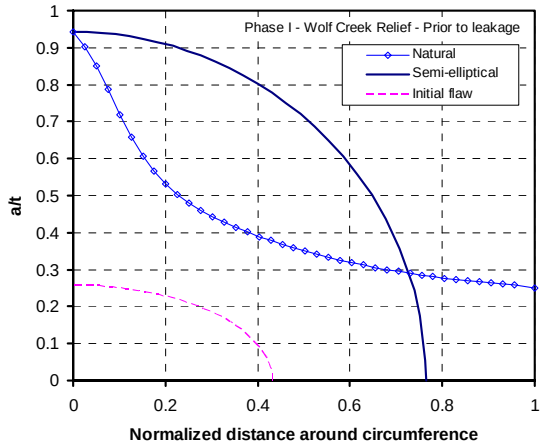

Figure 2 Crack shape prior to leakage assuming semi-elliptical crack growth and natural crack growth for relief nozzle geometry

The crack growth history for these cracks is shown in Figure 3. In this case, the solid lines represent the crack depth and the dashed lines represent the ID half crack length. The semi-elliptical solutions using the Anderson influence functions are shown in pink, while the arbitrary solutions using the PipeFracCAE software are shown in blue.

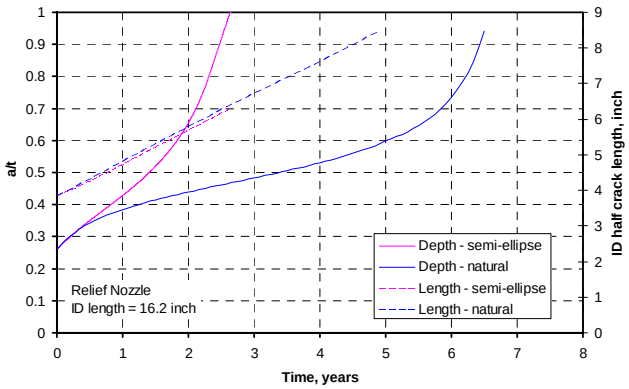

Figure 3 Time to through-wall penetration for relief nozzle case

As illustrated, not only is the margin on critical crack size affected, but the time to leakage is also under-estimated when the semi-elliptical assumption is used[†].

Currently, probabilistic piping fracture mechanics codes, such as PRO-LOCA [7] utilize the idealized surface crack solutions to estimate the probability of leakage in primary nuclear piping. As illustrated above, the use of the standard influence functions may be overly conservative from a leakage perspective for cracks that grow in an arbitrary manner. Therefore, in this effort, the PipeFracCAE code is used to determine the factors that drive a growing surface crack away from the semi-elliptical assumption. Sensitivity analyses are presented that compares the arbitrary crack growth behavior with that of the semi-elliptical crack growth behavior. The outcome of these analyses is a methodology to modify the standard influence functions, if necessary, to reduce the conservatism in predicting leakage from circumferentially orientated cracks growing by stress corrosion cracking mechanisms.

DESCRIPTION OF ANALYSES

In these analyses, three pipe sizes, typical for Westinghouse-type PWR primary piping, were chosen for this study. Table 1 shows the geometric details of the pipe sizes chosen. In this table, the large geometry corresponds to a typical hot leg, the medium corresponds to a typical surge line nozzle, and the small corresponds to typical relief line geometry.

Table 1 Geometry for sensitivity study

Pipe Geometry	D_o, mm (inch)	t, mm (in)	R_i/t
Small	197 (7.75)	32.8 (1.29)	2.00
Medium	381 (15.0)	40.1 (1.58)	3.75
Large	862 (33.94)	60.2 (2.37)	6.16

In addition to the geometry, three residual stress profiles (including a no residual stress case) were assumed, as illustrated in Figure 4. WRS1 and WRS2 both had an ID stress of 370 MPa (54 ksi), which represents the approximate value of the yield strength of as-welded Alloy 82/182 weld material. However, the difference between these profiles is that the

[†] As noted later in this paper, some of the differences in the plots are due to the curve fit of the Anderson solution.

WRS1 crosses into compression much deeper (as illustrated by X_c) in the wall than the WRS2 profile. Finally, the WRS3 profile has a much lower ID stress, and crosses into compression very close to the ID surface.

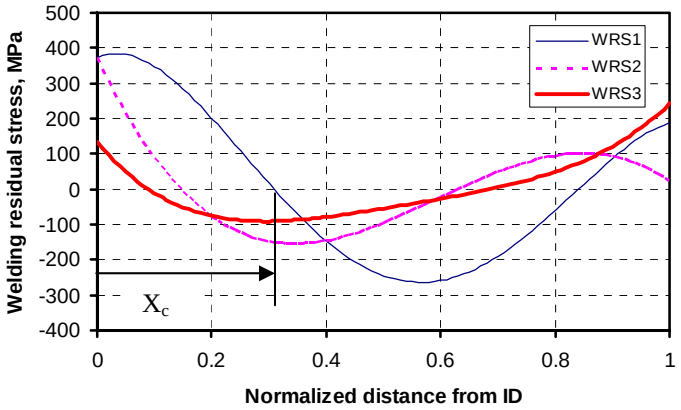

Figure 4 Welding residual stress profiles

Along with the welding residual stress, the normal operating loads were also varied in these analyses. The operating pressure (including crack face pressure) and axial load were held constant (15.4 MPa [2,235 psi], and 27.6 MPa [4 ksi] respectively), but the bending stress was varied between 43.5 MPa (6.3 ksi) [low bending] and 98.3 MPa (14.2 ksi) [high bending].

In most cases, the initial crack depth was held constant at 26% of the wall thickness, with the crack length set at 12.5% (short crack) and 40% (long crack) of the circumference. Several specific cases were conducted with a crack length of 25% (medium crack) of circumference. In addition, several small crack analyses, i.e., a/t=5%, θ/π = 1% (small crack), were conducted to investigate the crack size sensitivity. In all cases, the initial crack shape was semi-elliptical. In all, 53 analyses were completed in this investigation.

In this effort, the Alloy 82/182 PWSCC crack growth disposition curve developed by the nuclear industry [8] was used for all crack growth analyses. For the purposes of these analyses, the crack was assumed to propagate parallel to the dendrite grains and the temperature was assumed to be 644°F.

SHAPE FACTOR

In this effort, the evolution of the cracked area is used to compare the results. For these analyses, the cracked area is described by the shape factor (SF), which represents the area under the curves shown in Figure 5. This shape factor was tracked as a function of time for each analysis. In this figure, $t/t_{penetration}$ is the time normalized by the time at through-wall crack penetration. As illustrated in Figure 5 and Figure 6, the instantaneous cracked area was calculated for each simulation with PipeFracCAE, and output as a function of time. A shape factor of 0.785 represents a semi-ellipse. Therefore, the data generated can be compared with this value to determine if the flaws are naturally growing with a semi-elliptical shape. This comparison will add insight into how well the standard semi-elliptical influence functions may predict the leakage time and flaw size.

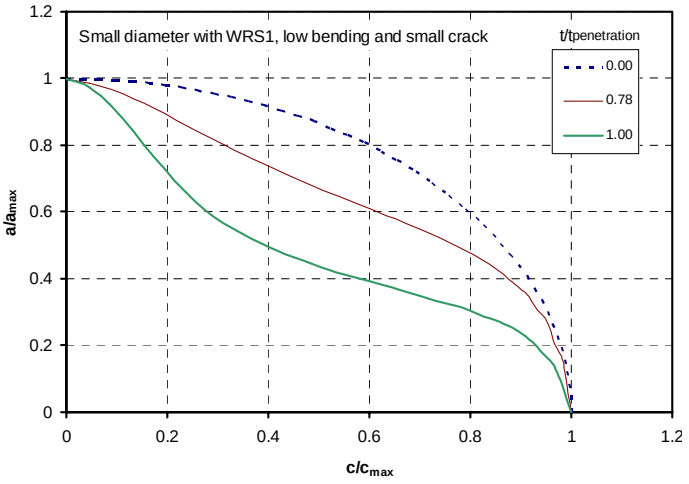

Figure 5 Normalized crack fronts to illustrate shape factor calculation

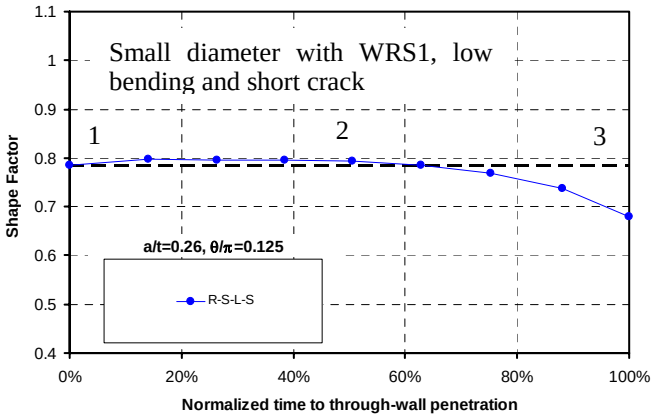

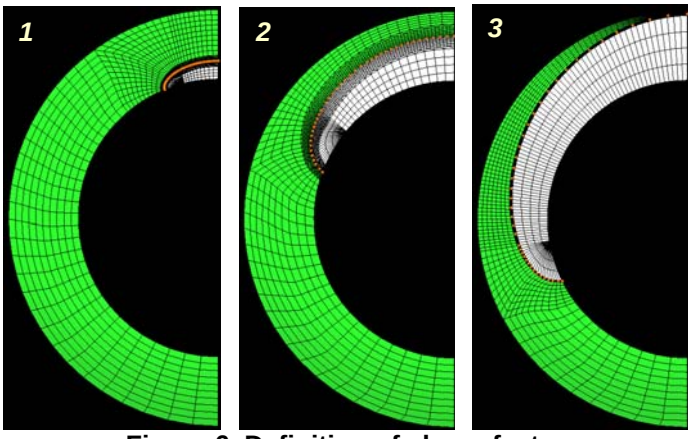

Figure 6 Definition of shape factor

RESULTS

As mentioned previously, 53 finite element analyses were completed to investigate the effects of welding residual stress, pipe size, crack size, and bending stress on the evolution of the surface crack shape. In all cases, the analyses were conducted until the arbitrary surface crack penetrated the wall and caused leakage. Through-wall crack analyses were not conducted in this investigation. The results in this paper are presented in two parts. First, the effects of these variables on the final crack shape will be discussed. Second, the ability of the standard

influence functions to predict the time to leakage and the crack length at leakage will be discussed.

Crack Shape at Leakage Results

In each of the cases described in this section, the plots presented represent the normalized final crack shape at the point of through-wall crack penetration. Therefore, the crack depth is normalized by the maximum crack depth along the crack front (a/a_{max}) and the crack length is normalized with the longest crack length along the crack front (c/c_{max}). In addition, the semi-elliptical crack front shape, which has a shape factor of 0.785, is shown for comparison purposes.

Figure 7 illustrates the effects of welding residual stress on the final crack shape. In this figure, the small diameter, low bending, short initial crack results are shown. The results from this figure suggests that the WRS3 has the largest effect on the final crack shape, with the WRS1 and no WRS giving about the same final crack shape. This comparison indicates that the X_c dimension from Figure 4 plays a large part in the development of the final crack shape. Also, WRS1 and WRS2 have the same ID stress, but significantly different X_c values. As illustrated by the crack shapes shown, the final crack length for these two cases are similar, but the shape factor at leakage is significantly different. Therefore, it appears that large values of X_c tend to drive the crack closer to semi-elliptically shaped. In fact, it appears that as X_c approached 0.4, the shape factor approaches that calculated when no WRS is considered.

Another interesting point from this figure is that case without WRS, even though it had about the same shape factor as the WRS1 case, had a much shorter crack length, which indicates that ID stress level is controlling the final crack length. Also, the no WRS case had a shape factor that was significantly lower (15%) than the original semi-elliptical case.

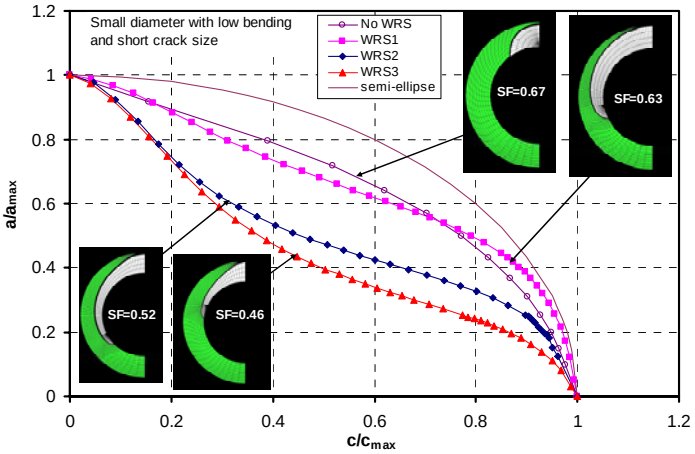

Figure 7 Effects of welding residual stress on final surface crack shape

The effects of initial crack size on the final crack shape are shown in Figure 8. In this case, the small diameter with WRS2 residual stress and low bending loads are shown. The three initial semi-elliptical crack shapes are

- Small crack: a/t=5% θ/π=1%
- Short crack: a/t=26% θ/π=12%
- Long crack: a/t=26% θ/π=40%

The results suggest that the initial crack shape has little influence (maximum 7%) on the final crack shape at leakage. In fact, as illustrated in Figure 9, the small crack growth history matches exactly the short crack growth history, once the small crack reaches the initial depth of the short crack. In this figure, the solid symbols are the short crack predictions, while the open symbols are the same predictions but shifted in time to the small crack curve.

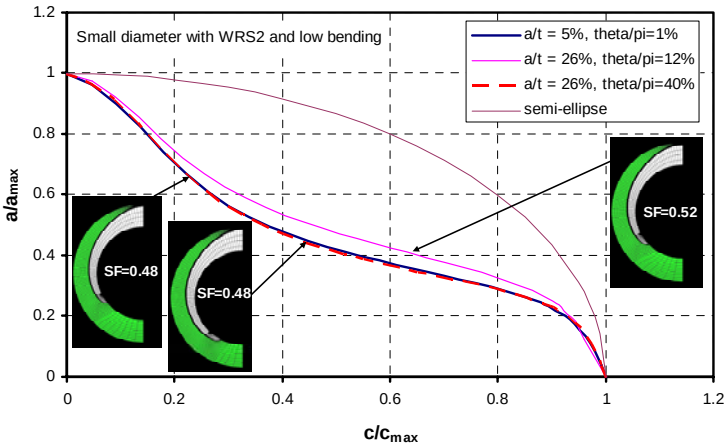

Figure 8 Effects of initial crack size on final shape

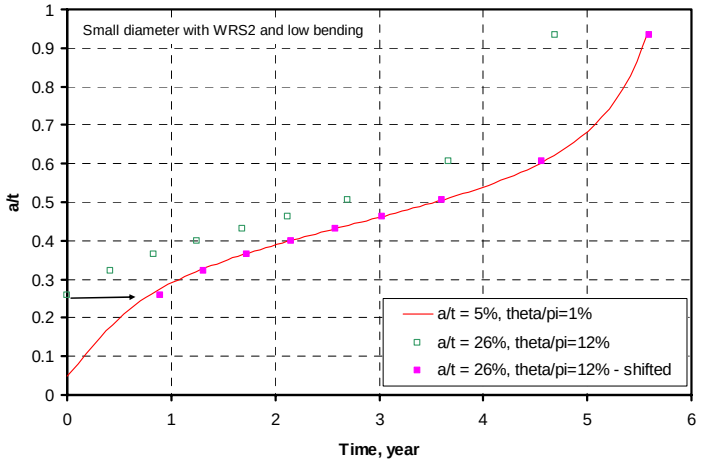

Figure 9 Crack growth comparison between small and short crack

The effects of diameter and R/t on the final crack shape are shown in Figure 10. As shown in this figure, the cases with the WRS2 welding stress, the low bending and short initial crack are shown. The diameter and R/t values used in these analyses are given in Table 1. The results in Figure 10 illustrate that the results are sensitive to diameter, with the crack in the smaller diameter having the smallest shape factor at leakage. In addition, due to the small circumference, the crack in the small diameter pipe extends 75% of the circumference, while in the large diameter pipe; the crack only extends 20% of the circumference. Therefore for the same stresses and initial relative crack size, the diameter and R/t have a large influence on the crack shape at leakage.

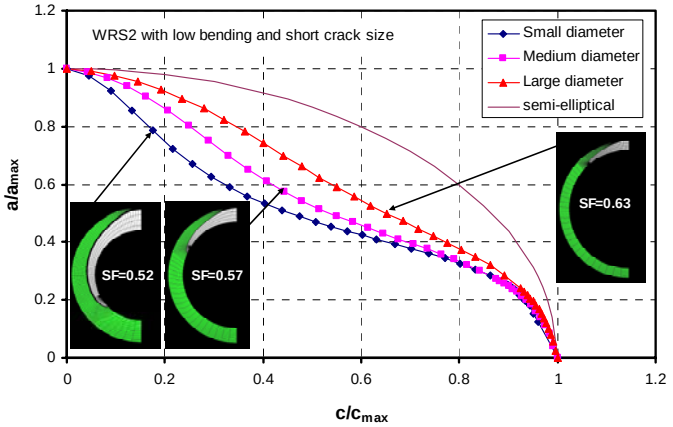

Figure 10 Effects of pipe diameter (R/t) on final crack shape

Finally, the effect of bending stress on the crack shape at leakage is illustrated in Figure 11. In this figure, the small diameter cases with the WRS2 residual stress and the short initial crack size are shown. As shown in this figure, the higher bending stress had a slightly larger shape factor than the low bending case. The larger difference is in the final crack length, with the low bending case extending 74% of the circumference, and the high bending extending 41% of the circumference. Therefore, the high bending pushes the crack through wall before the ID stress can contribute greatly to the crack length extension.

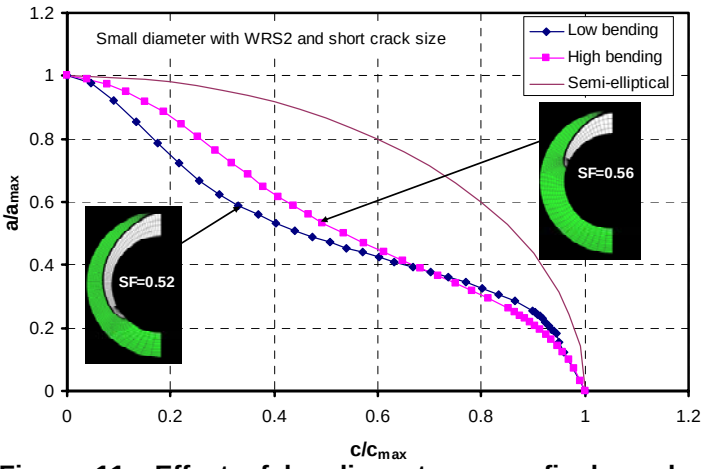

Figure 11 Effect of bending stress on final crack shape

It should be noted that the comparison of all 53 cases can not be shown here of sake of brevity, but the results presented here represent the trends observed in all cases.

PREDICATIONS OF TIME TO LEAKAGE AND FINAL CRACK LENGTH

From the previous discussion, the ID welding residual stress, the through-thickness location where the residual stress becomes compressive (X_c), the pipe geometry, and the bending stress level all contribute to the final crack shape at leakage. From a predictive standpoint, it is important to understand how well the standard influence functions for a semi-elliptical internal crack in a cylinder can be used to predict the arbitrary crack shapes that develop due to these complex stress fields.

In this effort, the Anderson influence functions [6] for an internal semi-elliptical surface crack in a cylinder were used for comparison to the PipeFracCAE results presented in the previous section. The Anderson solutions were developed from a series of finite element analyses for 4th-order stress distributions through the thickness with a/t from 0.2 to 0.8, c/a from 1 to 32 and R/t from 3 to 100. In this effort, a computer code was written to look up the influence functions from the tables in Reference 6 and linearly interpolate or extrapolate as necessary. The influence functions were calculated at the cracks deepest and surface point and the growth was calculated using the same growth law as described earlier. The cracks were assumed to remain semi-elliptical during the growth process.

Figure 12 shows the results of the time to leakage predictions with both the Anderson influence functions and calculated from PipeFracCAE when no welding residual stress is considered. In these cases, the geometry, crack size and bending are varied. As illustrated, the Anderson influence functions did an excellent job predicting the arbitrary crack leakage time. Note, that even though the shape factor for the cases with no welding stress (see Figure 7) was 15% lower than the semi-elliptical shape factor at leakage, the times at leakage were well predicted.

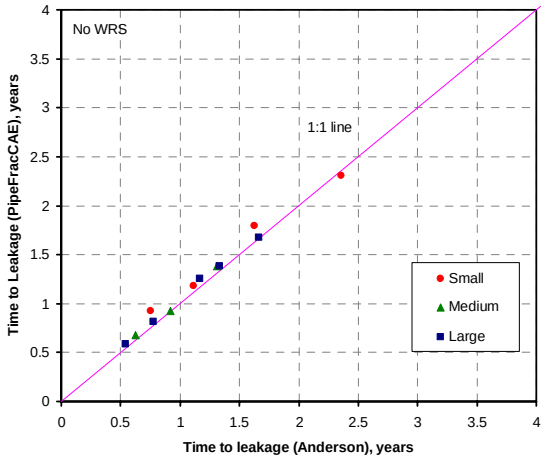

Figure 12 Predictions of time to leakage for cases with no welding residual stress

The same trend is true for the crack length predictions as shown in Figure 13. This figure shows the crack lengths at the time of the leakage predicted in Figure 12. As with the leakage times, the crack lengths are accurately predicted in all cases.

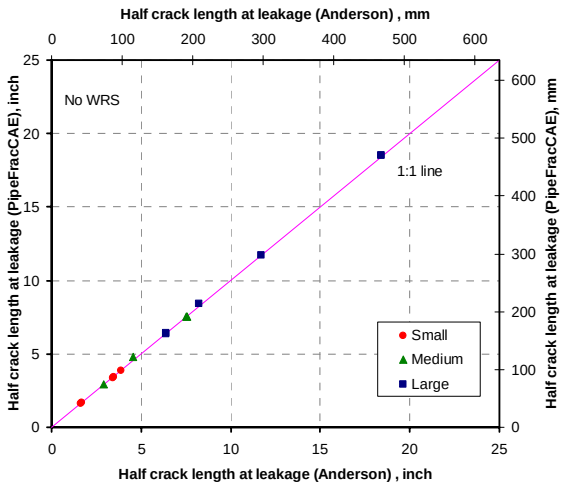

Figure 13 Predictions of crack length at leakage for cases with no welding residual stress

With the welding residual stress distributions included in the analyses, the predictions of time to leakage are shown in Figure 14, while the predictions of crack length at leakage are shown in Figure 15. The results from these figures suggest that the predictions using the Anderson influence functions are very accurate. In fact, on average, the time to leakage was low by 2% and the crack length was low by 3%.

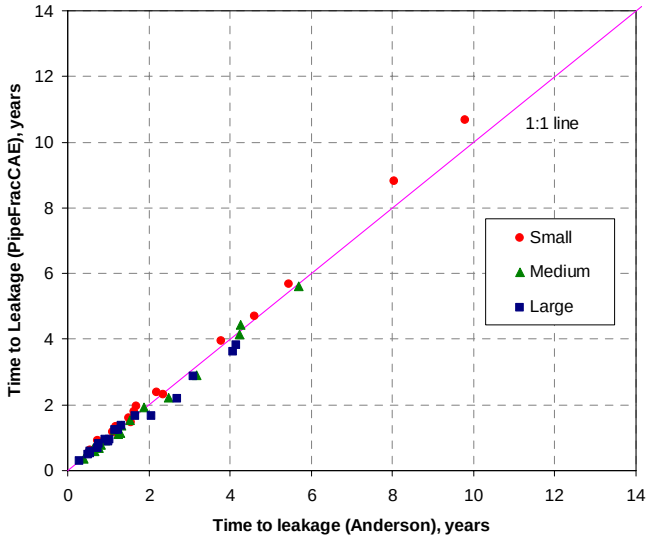

Figure 14 Predictions of time to leakage for cases with welding residual stress

These results are a bit surprising since in some cases the shape factor for the natural crack was up to 40% lower than a semi-ellipse. This fact suggests that the crack driving force is not highly driven by the overall crack shape, but more by just the length and depth of the crack.

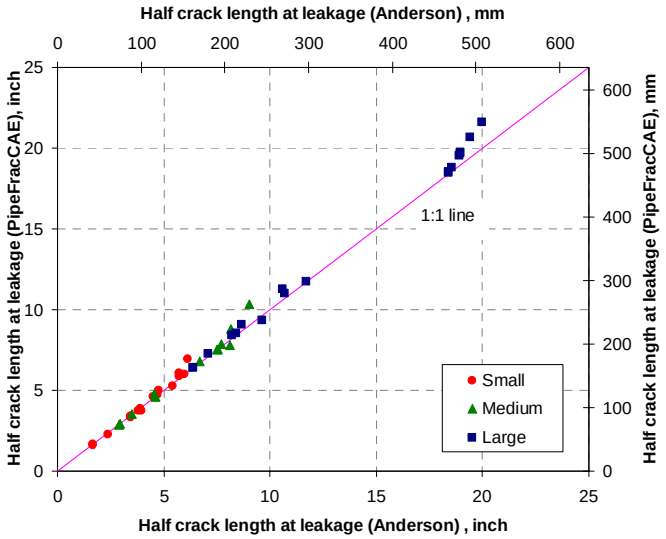

Figure 15 Predictions of crack length at leakage for cases with welding residual stress

DISCUSSION

The results presented in this paper appear contradictory to the results presented in Figure 3 and Reference 1, which suggest that the leakage predictions for the Wolf Creek relief line geometry using the Anderson influence functions severely underpredicted the time to leakage calculated with PipeFracCAE. However, in those initial analyses, a curve-fit solution to the Anderson influence functions was used. In the recent results presented in this paper, the influence function tables were used directly with linear interpolation and extrapolation used as needed. It was shown in previous reports [2,3] that the extrapolation using the curve fit solution was slightly inaccurate for the R/t values less than 3. As illustrated in Figure 16, when the look-up table is used, the predictions of leakage are very similar to those calculated with PipeFracCAE

This comparison illustrated the time-to-leakage sensitivity to the welding residual stresses. As discussed in Reference 3, the influence function predictions using the curve fits were not unreasonable, i.e., slope of the influence function predicted-to-actual line was 0.99 with a standard deviation of 2%. However, this difference was shown to have a large influence for the valleys of the WRS profile. As the crack reaches the area of maximum WRS compression, very small changes in the stress intensity factor can largely impact the time to leakage. Therefore, for accurate prediction, care must be taken in accurately capturing the WRS distribution, especially in the compressive region.

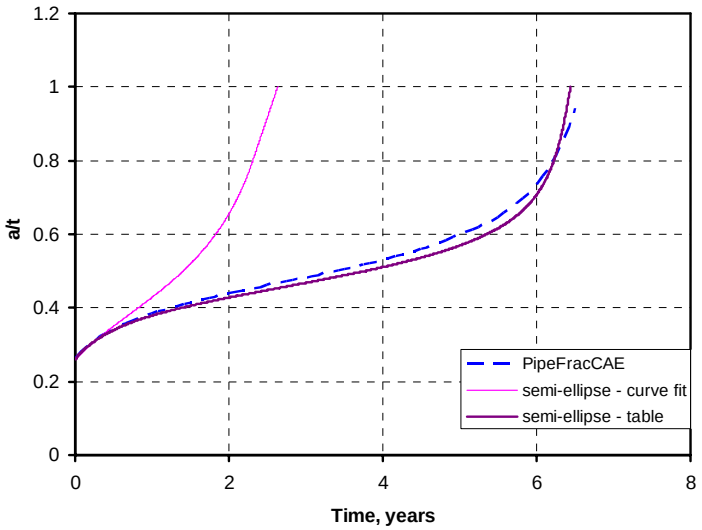

Figure 16 Predictions of leakage time for original Wolf Creek relief nozzle crack with influence function curve fit and look-up table

From this limited analysis set, it appears that the semi-elliptical surface crack influence functions can be used to accurately capture the time and crack length at through-wall crack penetration for cases with and without residual stress. However, the results suggest that the crack shape at leakage may be considerable different than the semi-elliptical or constant depth assumption typically used in these type of analyses. Using these idealized solutions for surface crack stability, leak rate predictions, or through-wall crack growth predictions may lead to overly conservative results.

It appears that the magnitude of the ID welding stress and the distance the welding stress crosses over into compression strongly influences the crack shape at leakage. Even though this was not an exhaustive study, the results presented here suggest that if the ID stress is on the level of the yield strength of the material, and X_c approaches 40% of the thickness, the crack shape approaches semi-elliptical. In addition, this effect is amplified if the bending stress is high and the diameter is large. This fact is illustrated in Figure 17. This case is for the larger diameter pipe with a short initial crack, with WRS1 residual stress and high bending stress. The final crack shape for this case is very close to semi-elliptical.

Having a high ID stress and a large X_c puts more of the cross section in tension, which produces a long crack with a high shape factor. Even though the time to leakage and crack length can be predicted with the semi-elliptical influence functions, the margin on critical crack size for the resulting leaking flaw will be worse than one generated with the same ID tensile stress but a much lower X_c. Therefore, the shape factor at leakage will need to be used in order to make an approximation of the through-wall cracked area for both leakage and stability analyses. Using the shape factor will help improve the through-wall crack stability and leakage calculations, but other information such as the OD crack length is needed before accurate leakage calculations can be made from these complex shaped cracks. Further investigation is needed before these trends can be defined.

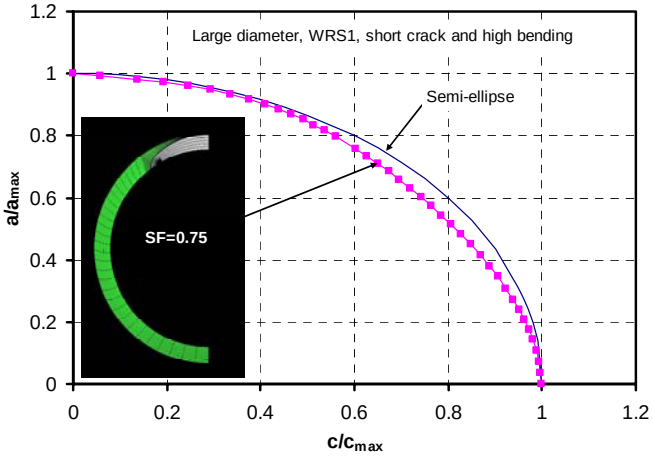

Figure 17 Example of case with semi-elliptical final crack shape

In all of these analyses, the crack is assumed to be planar, i.e., the crack remains in its initial plane. In reality, stress corrosion crack will tend to branch and "wander" away from the initial crack plane due to their intergranular behavior. These cracks will follow the path of greatest stress and least cracking resistance. Obviously, this behavior will affect the final crack front shape and is currently ignored in this investigation. In addition, such factors as uncertainties in crack growth rates and welding residual stress predictions will also affect these results. These factors are also ignored in this investigation.

One final point that needs to be addressed is that the WRS assumed in these analyses were axi-symmetric in nature, i.e., the WRS did not vary around the circumference. The evolution of the crack will be greatly affected if the WRS is not constant around the circumference, i.e., local repair weld. If an ID repair weld is present, past work [2, 3] has shown that the crack will be quickly driven through thickness and its length will extend to the length of the local repair. Further analyses are needed to determine the applicability of the semi-elliptical solutions for these conditions.

SUMMARY

In this paper, a series of advanced finite element analyses using the software PipeFracCAE were conducted to determine the effects of pipe geometry, operating loads, initial crack size and welding residual stress on the final surface crack shape at leakage. These arbitrary, or natural, crack analyses suggested that the ID tensile stress, the distance through-thickness the WRS crosses into compression and the pipe geometry greatly influence the final crack shape. It was illustrated that large diameter pipe with ID stresses at yield and large bending moments tend to produce cracks that are semi-elliptical at leakage. Most other cases will produce cracks that have less cracked area than a semi-elliptical crack with the same crack depth and length.

Even though the final cracked area from the natural crack analyses was less than the idealized semi-elliptical assumptions, the time to leakage and crack length at leakage predictions using the semi-elliptical solutions were very accurate. This result tends to suggest that crack driving force is more a function of the maximum crack depth and total length than the overall cracked area.

In addition to those factors presented in this paper, other issues such as non-planar crack growth, non-axi-symmetric welding residual stresses, and proper fitting of WRS distributions will all affect the predicted final crack shape. Further analyses are required before the effect of these factors can be quantified.

Finally, the final crack shape, i.e., shape factor, solutions can be used to further understand the true shape of the crack at first leakage. If these crack shapes can be correlated and predicted, accuracy of through-wall crack leakage and stability calculations can be greatly improved.

ACKNOWLEDGEMENTS

The authors would like to thank the Technical Advisory Group (TAG) members from the Battelle International group program MERIT (Maximizing Enhancement in Risk Informed Technology) for their support of this work. We would also like to thank Paul Scott of Battelle-Columbus, MERIT project manager, for his support of this project.

REFERENCES

1 Rudland, D.L., Shim, D.-J., Xu, H., and Wilkowski, G.W., "Evaluation of Circumferential Indications in Pressurizer Nozzle Dissimilar Metal Welds at the Wolf Creek Power Plant," Summary report to the NRC, April 2007. ADAMS ML071560398.

2 Materials Reliability Program: Advanced FEA Evaluation of Growth of Postulated Circumferential PWSCC Flaws in Pressurizer Nozzle Dissimilar Metal Welds (MRP-216, Rev. 1) EPRI, Palo Alto, CA: 2007. 1015383. MRP-216, Rev. 1.

3 Rudland, D.L., Shim, D.-J., Zhang, T., and Wilkowski, G., "Implications of Wolf Creek Indications – Final Report," Program final report to the NRC, August 2007. ADAMS ML072470394

4 ABAQUS Version 6.6-1. User's manual. ABAQUS, Inc., RI; 2006.

5 FEACrack, 3D Finite Element Software for Cracks, Version 3.0, Users Manual, Quest Reliability, Boulder Colorado, 2008.

6 Anderson, T.L., Thornwald, G., Revelle, D.A., and Lanaud, C., "Stress Intensity Solutions for Surface Cracks and Buried Cracks in Cylinders, Spheres, and Flat Plates," Structural Reliability Technology final report to The Materials Property Council, Inc., March 14, 2000.

7 Rudland, D., Xu, H., Wilkowski, G., Scott, P., Ghadiali, N., and Brust, F., "Development of a New Generation Computer Code (PRO-LOCA) for the Prediction of Break Probabilities for Commercial Nuclear Power Plants Loss-Of-Coolant Accidents," PVP2006-ICPVT11-93802, Proceedings of ASME-PVP 2006: 2006 ASME Pressure Vessels and Piping Division Conference, July 23-27, 2006,Vancouver, BC, Canada.

8 Materials Reliability Program (MRP) Crack Growth Rates for Evaluating Primary Water Stress Corrosion Cracking (PWSCC) of Alloy 82, 182, and 132 Welds (MRP-115), EPRI, Palo Alto, CA: 2004. 1006696.

